# Micropatterning of bioactive heparin-based hydrogels

**Sunny Satish Shah,†[a] Mihye Kim,†[b] Katelyn Cahill-Thompson,[a] Giyoong Tae*[b] and Alexander Revzin*[a]**

***Received 3rd August 2010, Accepted 5th November 2010***
**DOI: 10.1039/c0sm00771d**

This paper describes a UV photopatterning of bioactive heparin-based hydrogels on glass substrates. In this approach, hydrogel micropatterns were formed by UV-initiated thiol–ene reaction between thiolated heparin and diacrylated poly(ethylene) glycol (PEG-DA). Analysis of gelation kinetics showed that photo-crosslinked hydrogels formed faster and were stronger when compared to hydrogels formed by competing Michael addition reaction. To highlight bioactivity of heparin–PEG hybrid gels, hepatocyte growth factor (HGF) was mixed into prepolymer solution prior to hydrogel patterning. Immunostaining showed that HGF was retained after 5 days in the hybrid heparin–PEG hydrogel microstructures but was rapidly released from pure PEG gel microstructures. In a set of experiments further highlighting bioactivity of microfabricated heparin-based hydrogel, primary rat hepatocytes were cultured next to heparin and pure PEG hydrogel disks (~500 μm in diameter). ELISA analysis revealed that hepatocytes residing next to heparin-based hydrogels were producing ~4 times more albumin at day 7 compared to cells cultured next to inert PEG hydrogels. In the future, microfabricated heparin-based hydrogels described in this paper will be employed for designing cellular microenvironment *in vitro* and as vehicles for cell transplantation *in vivo*.



## Introduction

Cellular fate *in vivo* is shaped by interactions with neighboring cells, extracellular matrix (ECM) and signaling molecules (*e.g.* growth factors). It is important to mimic the complexity of these interactions in order to improve understanding of cues contributing to cell phenotype and to develop surrogate cell culture systems that better reflect complexity of native tissue.[1–3] Micropatterning approaches are particularly suited for designing and defining cell–microenvironment interactions. A number of such approaches have been described including microcontact printing,[4] photoresist lithography,[5–8] microfluidics,[9–11] protein microarrays[12–15] and electrochemical surface switching.[16–18]

Hydrogels are biomaterials that have been used extensively for designing cellular interactions *in vitro*.[19,20] Hydrogels may be broadly grouped into non-fouling and bio-functional categories. Non-fouling hydrogels are micropatterned to control cell–surface interactions[21–23] while biofunctional gels are being used for attachment/encapsulation of cells or controlled release of biomolecules.[19,20,24–27] Biofunctionalization of the gel typically involves incorporation of short peptide motifs to promote cell attachment or gel digestion. Recently, our laboratory described a new biofunctional hydrogel formed by Michael type addition reaction of thiolated heparin and acrylated poly(ethylene glycol) (PEG) chains.[28–30] Heparin is a glycosaminoglycan that is known to sequester various growth factors (GFs) and ECM proteins *via* secondary bond formation.[29,31,32] Unlike gels functionalized with short peptide motifs, our gel contained intact heparin molecules ($M_w$ 12 kDa) and proved to be an excellent matrix for GF release[29,33,34] and cell encapsulation/cultivation.[34,35]

While heparin-based hydrogel has shown considerable promise, Michael-type addition reaction used for gelation in our previous experiments was only suited for making large (millimetre-scale) gel objects.[36] Recently, Anseth and Salinas described thiol–ene reaction of thiolated biomolecules and acrylated PEG.[37,38] In the present paper, we investigated fabrication of heparin hydrogel microstructures using UV-initiated thiol–ene reaction of thiolated heparin (Hep-SH) and diacrylated PEG (PEG-DA) (see Fig. 1A for reaction scheme). Resultant hydrogel micropatterns were bioactive—retaining hepatocyte growth factor (HGF) after 5 days under physiological conditions and promoting function of primary rat hepatocytes. In the future, we envision using microfabricated heparin-based hydrogels in tissue engineering and stem cell differentiation studies.

## Experimental

### Chemicals and materials

Glass slides (75 × 25 mm) were obtained from VWR International, Inc. (Batavia, IL, USA). (3-Acryloxypropyl)trichlorosilane was purchased from Gelest, Inc. (Morrisville, PA, USA). Heparin (sodium salt, from porcine intestinal mucosa, $M_w$ 12 kDa) was purchased from Cellsus Ins. (Cincinnati, IA, USA). Poly(ethylene glycol) diacrylate (PEG-DA, $M_w$ 3.4 and 6 kDa, 98% degree of substitution) and tetra-functional poly(ethylene glycol) sulfhydryl (PEG-SH4, $M_w$ 10 kDa) were purchased from SunBio Inc. (Anyang, Korea). 4-(2-Hydroxyethoxy) phenyl-(2-hydroxy-2-propyl) ketone (Irgacure 2959) was purchased from Ciba Specialty Chemicals Inc. (Basel, Switzerland). Sulfuric acid, hydrogen peroxide, ethanol, epidermal growth factor (EGF), collagenase type IV, bovine serum albumin (BSA), hepatocyte growth factor (HGF), and toluidine blue O were purchased from

[a]*Department of Biomedical Engineering, University of California, Davis, 451 Health Sciences Dr. #2619, Davis, California, 95616, USA. E-mail: arevzin@ucdavis.edu*
[b]*Department of Materials Science and Engineering & Nanobio Materials and Electronics, Gwangju Institute of Science and Technology, Oryong-dong Buk-gu, Gwangju, 500-712, Korea. E-mail: gytae@gist.ac.kr*
† Equally contributing authors.

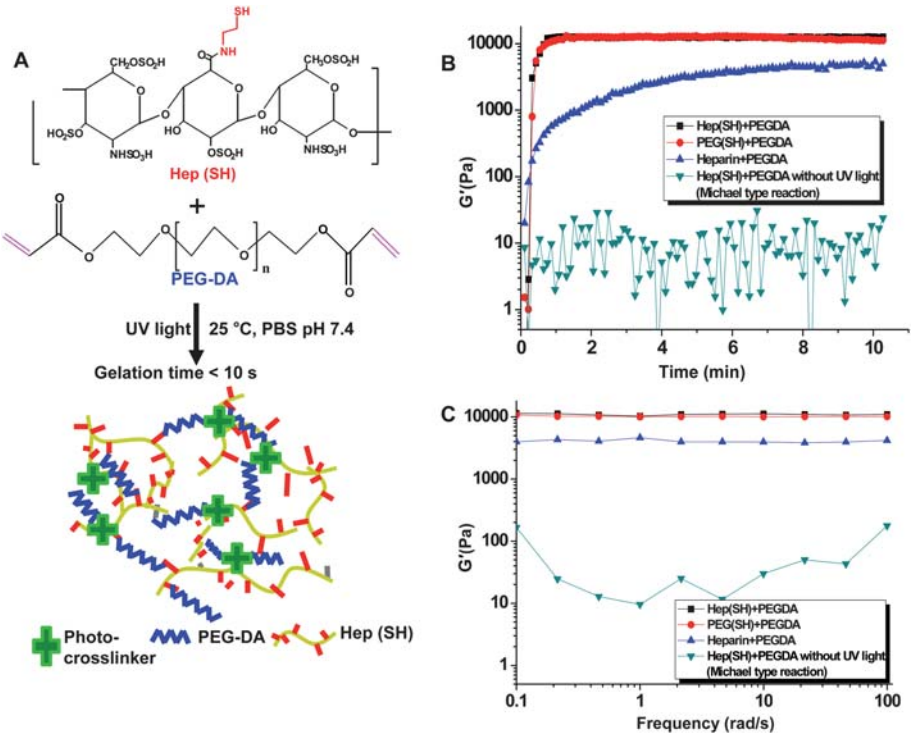


**Fig. 1** (A) Schematic representation of UV-initiated thiol–ene reaction between thiolated heparin and acrylated PEG. The gelation time for this polymerization reaction was less than 10 s. Gelation kinetics (B) and the final gel strengths (C) of hydrogels formed by UV photo-crosslinking: (■) heparin-based hydrogel formed with thiolated heparin and PEG-DA, (●) PEG hydrogel formed with 4-arm thiolated PEG and PEG-DA, (▲) PEG hydrogel containing physically incorporated heparin and PEG-DA, (▼) heparin-based hydrogel formed with thiolated heparin and PEG-DA by Michael type reaction without UV irradiation. Results show faster gelation of heparin hydrogel (■) and PEG hydrogel (●) formed by UV-initiated polymerization compared to Michael-type addition. In addition, heparin hydrogel (■) and PEG hydrogel (●) formed by photopolymerization were stronger compared to gels formed by Michael addition.

Sigma-Aldrich (St Louis, MO, USA). Glucagon and recombinant human insulin were obtained from Eli Lilly and Company (Indianapolis, IN, USA), and hydrocortisone sodium succinate was obtained from Pfizer Inc. (Ann Arbor, MI, USA). Concentrated phosphate-buffered saline (10× PBS) was purchased from Lonza (Walkersville, MD, USA). Dulbecco's modified Eagle's medium (DMEM), sodium pyruvate, nonessential amino acids, fetal bovine serum (FBS), and penicillin/streptomycin were purchased from Invitrogen (Carlsbad, CA, USA). Human HGF antibody and Goat IgG secondary antibody—H&L (HRP) were purchased from Abcam Inc. (Cambridge, MA, USA). Metal enhanced DAB substrate kit was obtained from Thermo Scientific Inc. (Rockford, IL, USA). Rat albumin ELISA kit was obtained from Bethyl Laboratories (Montgomery, TX, USA). Formalin was purchased from Fisher (Pittsburgh, PA, USA). Goat anti-rat IgG fluorescein isothiocyanate was purchased from Santa Cruz Biotechnologies, Inc. (Santa Cruz, CA, USA). Mounting medium with DAPI was purchased from Vector Laboratories, Inc. (Burlingame, CA, USA).

### Characterizing gelation kinetics

Gelation was characterized with respect to changes in rheological properties using a rheometer (Gemini, Malvern Instruments, UK). A transparent parallel plate geometry sample holder (gap: 0.3 mm and diameter: 15 mm) with a transparent solvent trap made of PMMA to allow UV irradiation but prevent drying during measurements and a roughened surface to prevent slippage of sample was used. An oscillatory time sweep at 1 rad $s^{-1}$ frequency for gelation kinetics, and a frequency sweep from 0.1 to 100 rad $s^{-1}$ with 1% shear strain in the linear viscoelastic range for gel strength after gelation were used. Under room temperature (25 °C), 60 μL of samples were loaded and exposed to 365 nm, 18 W $cm^{-2}$ UV light using an OmniCure series 1000 light source with an irradiation distance of 3 cm between the sample and the UV source. Gelation was subsequently characterized by monitoring the changes in elastic modulus (G′) at 25 °C controlled by a Peltier plate. The frequency sweep of the modulus at the final stage of polymerization was characterized to verify the gel formation. Gelation profiles for four different types of hydrogels were characterized: (1) heparin-based hydrogel formed by UV-initiated reaction of thiolated heparin (40% thiolation) and PEG-DA (6 kDa), (2) PEG hydrogel formed by UV-initiated reaction of 4-arm thiolated PEG (10 kDa) and PEG-DA (3.4 kDa), (3) hydrogel formed by UV-initiated polymerization of unmodified heparin and PEG-DA, and (4) hydrogel formed by Michael type reaction of thiolated heparin and PEG-DA by Michael type reaction without UV irradiation at 25 °C. Final concentration of hydrogel was 10% w/v in all cases. The four types of hydrogel were studied to determine: (a) the importance of thiolation for integration of heparin into hydrogel network—comparison of (1) and (3), (b) the possibility that Michael type

 

addition reaction was competing with UV-initiated thiol–ene reaction—comparison of (1) and (4), (c) the importance of heparin incorporation for bioactivity of hydrogel microstructures—comparison of bioactivity of (1) and (2). Control PEG hydrogels were prepared by using tetra-functional poly(ethylene glycol) sulfhydryl (PEG-SH4, 10 kDa) and 3.4 kDa PEG-DA (1 : 1 molar ratio of thiol group and acrylate group) with similar physical and mechanical properties to those of heparin-based hydrogels. In all cases, total concentration of gel precursors was set to be 10% w/v.

### Surface modification of glass substrate

Silane modification was used to anchor gel structures to glass. Glass slides were cleaned by immersion for 10 min in piranha solution consisting of three parts of sulfuric acid (95% v/v in water) and one part hydrogen peroxide (35% w/v in water). Glass slides were then thoroughly rinsed with deionized (DI) water, dried under nitrogen, and kept in a class 10000 clean room at room temperature. Prior to silane modification, the glass slides were treated in an oxygen plasma chamber (YES-R3, San Jose, CA, USA) at 300 W for 5 min. For silane modification, glass substrates were placed in 2 mM solution of 3-acryloxypropyl trichlorosilane in anhydrous toluene for 1 h. The reaction was performed in a glove bag under nitrogen purge to eliminate atmospheric moisture. After modification, the slides were rinsed with fresh toluene, dried under nitrogen, and cured at 100 °C for 2 h. Silane modified slides were placed in a desiccator until further use.

### Micropatterning of hydrogels on silane-modified glass surfaces

Heparin-based hydrogels were prepared by UV-initiated thiol–ene polymerization of thiolated heparin (Hep-SH) and diacrylated poly (ethylene glycol) (PEG-DA). 40% thiolated Hep-SH, prepared as reported previously,[30] and 6 kDa PEG-DA (1 : 1 molar ratio of thiol group and acrylate group) were dissolved in PBS containing 1% w/v photo-initiator, 4-(2-hydroxyethoxy) phenyl-(2-hydroxy-2-propyl) ketone (Irgacure 2959), in 70% v/v ethanol. This precursor solution was applied onto the silane-treated glass surface containing terminal acrylate functional groups and was covered with a cover slip (25 × 25 × 0.13 mm) to create a uniform prepolymer layer sandwiched between two glass substrates. Next, a photomask was placed on top of the liquid prepolymer layer and was exposed to 365 nm, 18 W $cm^{-2}$ UV light using an OmniCure series 1000 light source (EXFO, Vanier, Quebec, Canada). The regions exposed to UV light underwent polymerization and became cross-linked, while unexposed regions were dissolved after immersion in DI water. Manual dispensing of prepolymer allowed us to conserve custom-synthesized thiolated heparin (only 10 μl prepolymer solution is needed to micropattern 1 × 1 in glass piece). However, exposure of the prepolymer layer through a 130 μm thick glass cover slip limited hydrogel feature size to ~30 μm. Use of spin-coating and more precise control of the gap between photosensitive polymer and the photomask will allow us to decrease the feature size for hydrogel micropatterns in the future.

Toluidine blue O staining of hydrogel microstructures was performed as described by Gosey *et al.*[39] Staining of negatively charged heparin molecules in the hydrogel micropatterns by this dye (purple color) was visualized using optical microscopy (Zeiss Axiovert 40, Carl Zeiss, NJ, USA). Toluidine blue O staining was performed on three types of hydrogel micropatterns: (1) hydrogels created by UV-initiated thiol–ene reaction of Hep-SH and 6 kDa PEG-DA, (2) hydrogels created by free-radical polymerization of unmodified heparin ($M_w$ 12 kDa) and 6 kDa PEG-DA (same molar ratio of heparin and PEG-DA in case (1), and (3) hydrogels created by UV-initiated thiol–ene reaction of tetra-functional PEG-SH (10 kDa) and 3.4 kDa PEG-DA (1 : 1 molar ratio of thiol group and acrylate group). These three types of hydrogels had similar mechanical properties[33] but differed in terms of the presence of heparin molecules and their covalent integration into the gel. In all cases, total concentration of gel precursors was set to be 10% w/v.

### HGF retention in hydrogel microstructure

Equal amounts of 20% w/v hydrogel and 1 mg $mL^{-1}$ HGF were mixed to form a final concentration of 10% w/v hydrogel containing 0.5 mg $mL^{-1}$ HGF. Two types of precursor solutions were used: (1) heparin-based hydrogel formed with thiolated heparin (40% thiolation) and PEG-DA (6 kDa) and (2) PEG hydrogel formed with 4-arm thiolated PEG (10 kDa) and PEG-DA (3.4 kDa). Hydrogel micropatterns were prepared on glass substrates as described in the previous section and were stored at 37 °C in 1× PBS for up to 5 days. The hydrogel micropatterns were immunostained at days 1 and 5 to check the amount of retained HGF. First, samples were incubated with the human HGF antibody (diluted 1 : 2000 in blocking solution) for 2 h at 37 °C and washed twice in 1× PBS solution. Next, samples were incubated with Goat IgG secondary antibody—H&L (HRP) (diluted 1 : 5000 in blocking solution) for 1 h at room temperature followed by washing in PBS solution. To visualize the presence of HGF, a DAB (3,3′diaminobezidine) color reagent (Thermo Scientific Inc. Rockford, IL, USA) was diluted 1 : 10 in peroxide buffer and incubated with hydrogel micropatterns for 10 min at room temperature in the dark Brown color due to HGF immunostaining was observed by brightfield microscopy.

### Cell patterning around heparin-hydrogel microstructures

Primary rat hepatocytes were employed in our studies. Cells were isolated from adult female Lewis rats (Charles River Laboratories, Boston, MA) weighing 125–200 g, using a two-step collagenase perfusion procedure described previously.[40] Typically, 100–200 million hepatocytes were obtained with viability >90% as determined by trypan blue exclusion. Primary hepatocytes were maintained in DMEM supplemented with epidermal growth factor (EGF), glucagon, hydrocortisone sodium succinate, recombinant human insulin, 200 units per mL penicillin, 200 μg $mL^{-1}$ streptomycin and 10% FBS. Prior to cell seeding, hydrogel micropatterns were formed on silane-coated glass substrates using the protocol described earlier. The substrates were then incubated with collagen I solution (0.1 mg $mL^{-1}$) for 20 minutes, washed in 1× PBS solution, rinsed in DI water and dried using nitrogen. The surfaces were placed into a 12-well plate and exposed to 3 mL of rat primary hepatocytes suspended in culture medium at a concentration of 1 × $10^6$ cells $mL^{-1}$. After

1 h of incubation at 37 °C, hepatocytes became localized on collagen regions, but did not attach on top of the hydrogel. The samples were then washed twice in PBS to remove unbound hepatocytes and fresh media were added to the sample well. Murine 3T3 fibroblasts were maintained in DMEM supplemented with 10% FBS, 200 U $mL^{-1}$ penicillin, and 200 μg $mL^{-1}$ streptomycin at 37 °C in a humidified 5% $CO_2$ atmosphere. 3T3 cells were seeded using the same protocol as described above.

### Analysis of hepatic function

Production of albumin by the hepatocytes was assessed using standard ELISA protocols.[40] To detect intracellular albumin, samples with primary hepatocytes were placed into 4% formalin solution and were subsequently washed three times in 1× PBS solution. The samples were then incubated with anti-rat serum albumin antibody (1 : 250 dilution in 1× PBS) for 1 h at room temperature. After incubation, samples were washed twice in 1× PBS solution. The samples were then stained with anti-sheep IgG conjugated with fluorescein isothiocyanate (1 : 100 dilution in 1× PBS) for 1 h at room temperature followed by a two-time rinse in 1× PBS solution. Finally, samples were mounted using a mounting medium containing DAPI to determine the location of nuclei. Stained cells were visualized and imaged using a confocal microscope.

## Results and discussion

In this study, we describe microfabrication of bioactive heparin-containing hydrogels (Fig. 1). Gelation kinetics were characterized and micropatterning of hydrogel structures of varying geometries was demonstrated. Primary hepatocytes cultured for 7 days next to heparin hydrogel micropatterns produced much higher levels of albumin compared to cells cultured next to inert PEG micropatterns.

### Gelation kinetics of heparin hydrogel

The gelation kinetics were characterized by monitoring the changes in elastic modulus ($G'$) with a rheometer. Gelation profiles of four types of materials were studied: (1) heparin-based hydrogel formed with thiolated heparin and PEG-DA, (2) PEG hydrogel formed with 4-arm thiolated PEG and PEG-DA, (3) hydrogel formed with unmodified heparin and PEG-DA, and (4) heparin-based hydrogel formed with thiolated heparin and PEG-DA by Michael type reaction without UV irradiation. As shown in Fig. 1B, at a fixed irradiation time (1 min at UV intensity of 18 W $cm^{-2}$) and initiator concentration (1% w/v), fast and intense crosslinking was achieved for cases (1) and (2) due to the photoinitiated polymerization between acrylate and thiol groups. When unmodified heparin was used instead of thiolated heparin, only PEG-DA molecules underwent free radical polymerization resulting in slower gelation. Experiments described in Fig. 1 were carried out at 25 °C, below the temperature needed for Michael-type addition reaction.[30] Therefore, as shown in Fig. 1B, UV-initiated gelation of acrylated and thiolated precursors occurred as fast as 10 s (cases 1 and 2) whereas no appreciable gelation was seen after 10 min of Michael addition reaction (case 4). These data suggested that at room temperature, with UV initiation, thiol–ene reaction was the predominant mode of gel formation.

Analysis of mechanical properties (Fig. 1C) showed that UV-initiated polymerization of precursor solutions of thiolated heparin/acrylated PEG (case 1) and thiolated PEG/acrylated PEG (case 2) resulted in strongly networked gel with a storage modulus of ~11 kPa. On the other hand, UV polymerization of unmodified heparin/acrylated PEG solution resulted in a weaker gel of ~0.4 kPa. This suggests that unmodified heparin was not covalently linked into the gel network. Lack of integration of unmodified heparin into the gel was further confirmed by heparin staining discussed in the next section. Fig. 1C also shows that gel formation did not occur *via* Michael type addition reaction of thiolated heparin and acrylated PEG when carried out at room temperature.

The concentration and the composition of the heparin hydrogel have been shown by us to have a significant impact on the bioactivity of the hydrogel.[30,35] The hydrogel modulus could be controlled by the total concentration of precursors, the degree of thiolation of Hep-SH, the molecular weight of PEG-DA and the molar ratio between two precursors. Gels with modulus similar to that of native tissue (liver) were shown to elicit highest levels of hepatic phenotype expression. We also hypothesize that increasing the molar fraction of heparin in the hydrogel may further increase the biological activity of the hydrogels.

### Formation of hydrogel micropatterns

Fast gel formation allowed to micropattern heparin-containing prepolymer solution in a manner analogous to negative tone resist lithography. As described in Fig. 2A, liquid prepolymer solution was dispensed onto a glass substrate and exposed to UV through a photomask, resulting in thiol–ene cross-linking of exposed regions. Unpolymerized precursor solution was removed by development in water, leaving behind hydrogel microstructures anchored to glass substrate. Attachment of hydrogels to glass was achieved *via* an acrylated silane coupling layer described by us previously.[8,21]

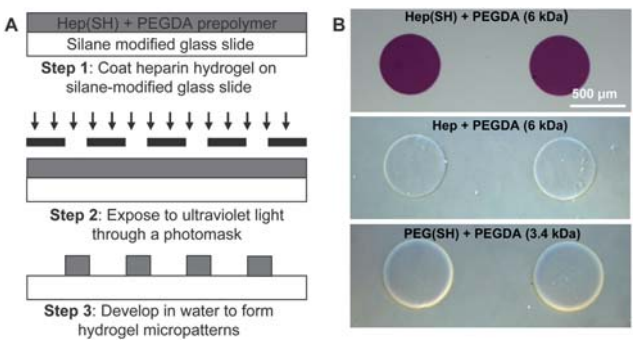


**Fig. 2** (A) Diagram describing micropatterning of heparin-based hydrogel. After coating silane-modified glass with heparin-based PEG prepolymer solution, the substrate was exposed to UV light through a photomask, crosslinking exposed regions. Unexposed regions of the precursor solution were developed by immersion in water. (B) Heparin-based hydrogel formed by UV-initiated thiol–ene reaction stained for negatively charged heparin molecules by toluidine blue O (upper panel). Hydrogel with physically incorporated heparin (middle panel) or no heparin (lower panel) did not retain toluidine blue O. These data suggest that UV-initiated thiol–ene reaction allowed integration of heparin into hydrogel network.

 

The presence of heparin in the hydrogel microstructures was confirmed by toluidine blue O staining. This dye has a positive charge[39] and binds strongly to negatively charged heparin molecules. As shown in Fig. 2B (upper panel), the heparin-based hydrogel, formed by UV-initiated exposure of thiolated heparin and PEG-diacrylate precursors, retained toluidine blue O dye (red/purple color), indicating that heparin was present in the hydrogel. Conversely, toluidine blue O staining was not observed in the gel formed by photocrosslinking of unmodified heparin/PEG acrylate precursor solution (Fig. 2B, middle panel), suggesting unmodified heparin leached out after immersion of gel structures in water. Pure PEG hydrogels serving as negative control also showed lack of toluidine blue O staining (Fig. 2B, lower panel). These results suggest that only thiolated heparin was stably/covalently incorporated into hydrogel microstructures.

Importantly, photolithography approach described here allowed fabrication of hydrogel microstructures of various dimensions and geometries. Fig. 3 shows a range of sizes and geometries of heparin-based hydrogel microstructures photolithographically patterned on glass. Toluidine blue O staining (purple color) demonstrates the presence of heparin inside these hydrogel micropatterns.

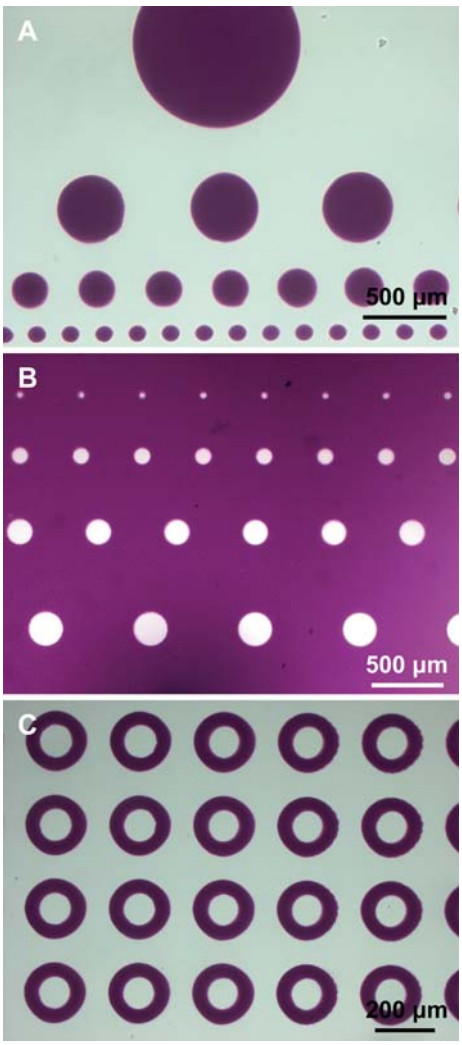


**Fig. 3** Micropatterning of heparin hydrogel structures of varying geometries on a glass substrate. Disks (A), microwells (B) or rings (C) could be microfabricated with ease based on the design of the photomask. Toluidine blue O staining (purple color) shows the presence of negatively charged heparin molecules inside the hydrogel.

### Retention of HGF in heparin hydrogel microstructures

A number of microfabricated gels have been described in the literature.[20,21,23,41–43] Unlike these previous reports, microfabricated hydrogels described in this study contained intact heparin—a 12 kDa glycosaminoglycan that associates with proteins *via* heparin binding domains. HGF is a heparin binding domain-expressing protein that is involved in the development/regeneration of liver as well as other organs.[44,45] To highlight the bioactivity of microfabricated hydrogels, HGF was added into prepolymer solutions of either thiolated heparin/acrylated PEG or thiolated PEG/PEG-DA. After micropatterning, hydrogel structures prepared from these two prepolymer solutions were immunostained for the presence of HGF. HRP-labeled antibodies and precipitating reagent DAB were used to visualize retention of HGF molecules in the hydrogel. Fig. 4 shows that HGF is present in both heparin-containing and heparin-free hydrogel microstructures (brown color) after one day incubation of micropatterned surface under physiological conditions. By day five, however, heparin-based gel microstructures retained HGF, whereas HGF staining of pure PEG microstructures was approaching that of a negative control (gels without HGF). This supports the notion that heparin hydrogel microstructures can bind GFs to ensure slower/more sustained release of these molecules.

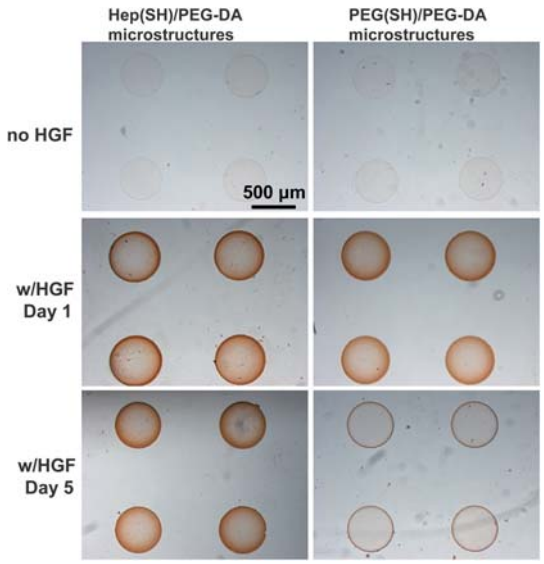


**Fig. 4** HGF retention inside hydrogel microstructures. HGF was incorporated into prepolymer solution comprised of either thiolated heparin/PEG-DA or thiolated PEG/PEG-DA. The resultant hydrogel micropatterns were immunostained for HGF with HRP/DAB amplification used to visualize signal (brown color). Results show that at day 1, both heparin-based and all PEG hydrogels stained strongly for HGF, however, by day 5 only heparin-based gel microstructures retained HGF.

### Cultivating cells on surfaces containing hydrogel microstructures

In order to further assess the bioactivity of heparin gel, primary rat hepatocytes were cultured on glass substrates containing hydrogel micropatterns. To promote cell attachment, micropatterned surfaces were incubated for ~20 min in solution of collagen (I). Given that heparin-containing hydrogels had high PEG content (1 : 1 molar ratio of heparin to PEG), this short incubation was sufficient to deposit collagen on silanized glass but was insufficient to adsorb protein molecules onto the hydrogel. Immersion of micropatterned surfaces into collagen (I) solution ensured that cells attached onto regions around or within but not on top of hydrogel structures. We do envision culturing cells either on top or inside hydrogel microstructures as described in our recent publications,[35,36] however, in this study we wanted to assess proximity or paracrine effects of heparin gel microstructures on neighboring cells.

Fig. 5A and B show representative images of hepatocytes adherent next to hydrogel microstructures (wells and pillars), while Fig. 5C demonstrates patterning of stromal cells (3T3 fibroblasts). Higher magnification image in Fig. 6A shows that hepatocytes residing next to heparin hydrogel structures had cuboidal morphology with large nuclei and prominent cell–cell boundaries—features consistent with differentiated hepatic phenotype. *In vivo*, liver is responsible for synthesis of serum proteins such as albumin. Therefore, albumin synthesis is used as one measure of hepatocyte function *in vitro*. Immunostaining for intracellular albumin was carried out to characterize functionality of hepatocytes. Fig. 6B shows strong signal associated with the presence of albumin in the cytoplasm of hepatocytes (green fluorescence) residing next to heparin hydrogel microstructures. A weak intracellular albumin signal was observed in cells cultured next to pure PEG gel structures (data not shown).

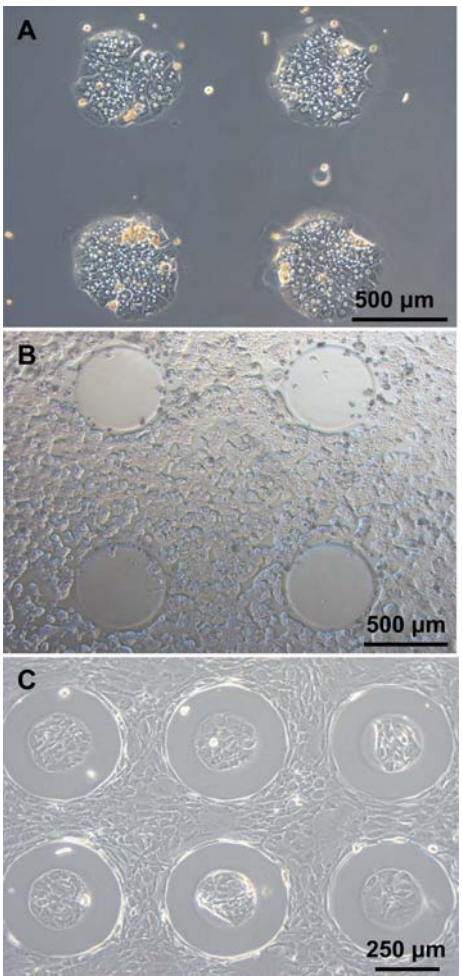


**Fig. 5** Micropatterning of cells on hydrogel containing surfaces. (A) Primary rat hepatocytes residing inside heparin hydrogel microwells and (B) around hydrogel disks. (C) Patterning of 3T3 fibroblasts around heparin hydrogel ring structures.

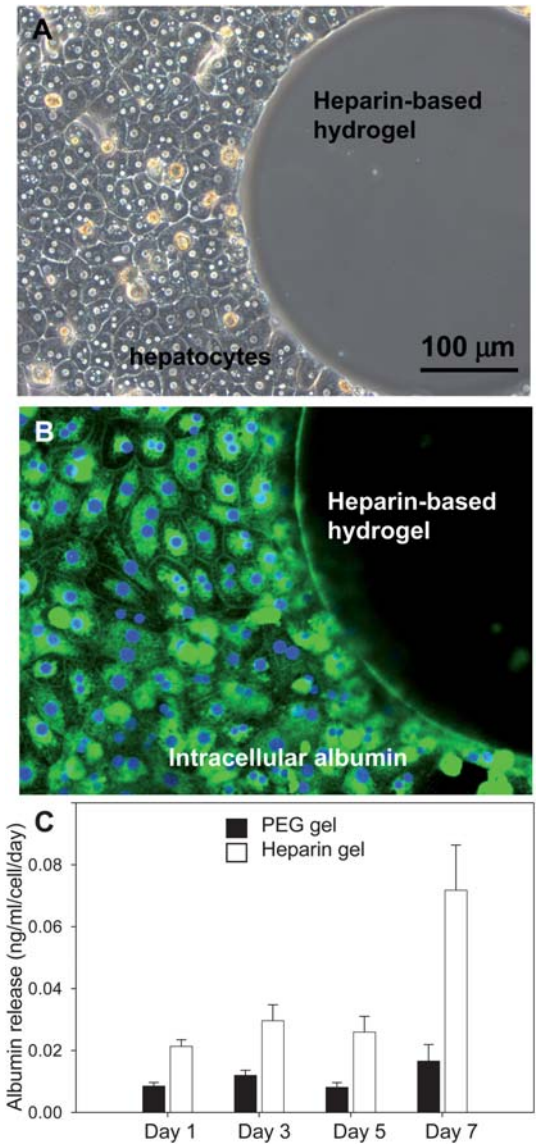


**Fig. 6** Bioactivity of hydrogel microstructures. (A) Brightfield microscopy image showing cuboidal morphology of primary rat hepatocytes. (B) Intracellular albumin immunostaining of primary hepatocytes residing next to heparin-based hydrogel element at day 6 in culture. Green color—intracellular albumin and blue color—DAPI staining of nuclei. (C) ELISA analysis of albumin secretion by primary hepatocytes cultured next to PEG and heparin-based hydrogel micropatterns. Error bars represent standard deviation of the mean for $n = 3$ samples.

Additional proof of enhancement in the function of hepatocytes residing next to heparin hydrogel surfaces was obtained by albumin ELISA. As seen in Fig. 6C, albumin production in hepatocytes cultured next to heparin-based hydrogel microstructures was 4 fold higher at day 7 compared to hepatocytes cultured next to pure PEG hydrogels. Albumin secretion level of 0.075 ng $mL^{-1}$ per cell per day in hepatocytes residing next to heparin hydrogels was 2 to 4 fold lower than in micropatterned co-cultures but still significantly higher than albumin synthesis reported for hepatocyte monocultures.[46,47] Significant enhancement in hepatic function observed in Fig. 6 may be attributed to cells being stimulated by biomolecules released from heparin hydrogels. It should be noted that heparin hydrogels were not preloaded with HGF or other biomolecules; therefore, gel bioactivity should be attributed to uptake and release of signaling molecules present in cell culture. While the hepatostimulatory signals released by the hydrogel are yet to be determined, one possible mechanism is that heparin gel structures take up cell-secreted molecules at initial stages of cultivation and release these molecules back to cells over time in culture, thus preventing de-differentiation of hepatocytes. This and other mechanisms explaining the bioactivity of heparin hydrogels are currently under investigation in our laboratories.

## Conclusion

While a large number of hydrogel types and microfabrication strategies have been described in the literature, the reports on microfabricated gels that actively stimulate and promote cell function are limited. In this study, we describe photo-patterning of thiolated heparin and diacrylated PEG to create hydrogel microstructures with covalently incorporated heparin domains. Dynamics of polymerization were characterized, showing that photo-initiated gelation was several fold faster than competing Michael addition reaction. Using photolithography-like process, we fabricated heparin hydrogel microstructures of varying geometries and dimensions. Importantly, hydrogel microstructures were bioactive—allowing controlled release of HGF and promoting the function of primary rat hepatocytes. We envision future use of microfabricated heparin-based gels in designing tissue engineered constructs, promoting differentiation of stem cells and developing vehicles for stem cell transplantation.

## Acknowledgements

The authors would like to thank Dr Caroline Jones for isolating primary rat hepatocytes. The authors would also like to thank Prof. Louie's laboratory at UC Davis for use of confocal microscopy. S.S.S. was supported by grant number T32-GM08799 from NIGMS-NIH. G.T. acknowledges support from World Class University (WCU) program at GIST through a grant provided by the Ministry of Education, Science and Technology (MEST) of Korea (Project No. R31-20008-000-10026-0) and by the Research Center for Biomolecular Nanotechnology, GIST. A.R. acknowledges support from NIH (R01DK079977).

## References

1 A. Folch and M. Toner, *Annu. Rev. Biomed. Eng.*, 2000, **2**, 227.
2 J. El-Ali, P. K. Sorger and K. F. Jensen, *Nature*, 2006, **442**, 403–411.
3 A. Khademhosseini, R. Langer, J. Borenstein and J. P. Vacanti, *Proc. Natl. Acad. Sci. U. S. A.*, 2006, **103**, 2480–2487.
4 G. M. Whitesides, E. Ostuni, S. Takayama, X. Jiang and D. E. Ingber, *Annu. Rev. Biomed. Eng.*, 2001, **3**, 335–373.
5 S. N. Bhatia, M. L. Yarmush and M. Toner, *J. Biomed. Mater. Res.*, 1997, **34**, 189–199.
6 E. E. Hui and S. N. Bhatia, *Langmuir*, 2007, **23**, 4103–4107.
7 J. Y. Lee, C. Zimmer, G. Y. Liu and A. Revzin, *Langmuir*, 2008, **24**, 2232–2239.
8 J. Y. Lee, S. S. Shah, J. Yan, M. C. Howland, A. N. Parikh, T. R. Pan and A. Revzin, *Langmuir*, 2009, **25**, 3880–3886.
9 S. Takayama, J. C. McDonald, E. Ostuni, M. N. Liang, P. J. A. Kenis, R. F. Ismagilov and G. M. Whitesides, *Proc. Natl. Acad. Sci. U. S. A.*, 1999, **96**, 5545–5548.
10 B. G. Chung, L. A. Flanagan, S. W. Rhee, P. H. Schwartz, A. P. Lee, E. S. Monuki and N. L. Jeon, *Lab Chip*, 2005, **5**, 401–405.
11 U. Y. Schaff, M. M. Q. Xing, K. K. Lin, N. Pan, N. L. Jeon and S. I. Simon, *Lab Chip*, 2007, **7**, 448–456.
12 C. J. Flaim, S. Chien and S. N. Bhatia, *Nat. Methods*, 2005, **3**, 119.
13 Y. Soen, A. Mori, T. D. Palmer and P. O. Brown, *Mol. Syst. Biol.*, 2006, **2**, 37.
14 C. N. Jones, N. Tuleuova, J. Y. Lee, E. Ramanculov, A. H. Reddi, M. A. Zern and A. Revzin, *Biomaterials*, 2009, **30**, 3733–3741.
15 C. N. Jones, N. Tuleuova, J. Y. Lee, E. Ramanculov, A. H. Reddi, M. A. Zern and A. Revzin, *Biomaterials*, 2010, **31**, 5936–5944.
16 M. N. Yousaf, B. T. Houseman and M. Mrksich, *Proc. Natl. Acad. Sci. U. S. A.*, 2001, **98**, 5992–5996.
17 E. W. L. Chan, S. Park and M. N. Yousaf, *Angew. Chem., Int. Ed.*, 2008, **47**, 6267–6271.
18 S. S. Shah, J. Y. Lee, S. Verkhoturov, N. Tuleuova, E. A. Schweikert and A. Revzin, *Langmuir*, 2008, **24**, 6837–6844.
19 M. P. Lutolf and J. A. Hubbell, *Nat. Biotechnol.*, 2005, **23**, 47–55.
20 V. L. Tsang, A. A. Chen, L. M. Cho, K. D. Jadin, R. L. Sah, S. DeLong, J. L. West and S. N. Bhatia, *FASEB J.*, 2007, **21**, 790–781.
21 A. Revzin, R. G. Tompkins and M. Toner, *Langmuir*, 2003, **19**, 9855–9862.
22 K. Y. Suh, J. Seong, A. Khademhosseini, P. E. Laibinis and R. Langer, *Biomaterials*, 2004, **25**, 557–563.
23 M. Charnley, M. Textor, A. Khademhosseini and M. P. Lutolf, *Integr. Biol.*, 2009, **1**, 625–634.
24 M. P. Lutolf, J. L. Lauer-Fields, H. G. Schmoekel, A. T. Metters, F. E. Weber, G. B. Fields and J. A. Hubbell, *Proc. Natl. Acad. Sci. U. S. A.*, 2003, **2003**, 5413–5418.
25 M. P. Lutolf, G. P. Raeber, A. H. Zisch, N. Tirelli and J. A. Hubbell, *Adv. Mater.*, 2003, **15**, 888–892.
26 A. H. Zisch, M. P. Lutolf, M. Ehrbar, G. P. Raeber, S. C. Rizzi, N. Davies, H. Schmokel, D. Bezuidenhout, V. Djonov, P. Zilla and J. A. Hubbell, *FASEB J.*, 2003, **17**, 2260–2262.
27 J. J. Moon, M. S. Hahn, I. Kim, B. A. Nsiah and J. L. West, *Tissue Eng., Part A*, 2009, **15**, 579–585.
28 G. Tae, J. A. Kornfield and J. A. Hubbell, *Biomaterials*, 2005, **26**, 5259–5266.
29 G. Tae, M. Scatena, P. S. Stayton and A. S. Hoffman, *J. Biomater. Sci., Polym. Ed.*, 2006, **17**, 187–197.
30 G. Tae, Y. J. Kim, W. I. Choi, M. Kim, P. S. Stayton and A. S. Hoffman, *Biomacromolecules*, 2007, **8**, 1979–1986.
31 I. Capila and R. J. Linhardt, *Angew. Chem., Int. Ed.*, 2002, **41**, 391–412.
32 S. Ashikari-Hada, H. Habuch, Y. Kariya, N. Itoh, A. H. Reddi and K. Kimata, *J. Biochem.*, 2004, **279**, 12346–12354.
33 W. I. Choi, M. Kim, G. Tae and Y. H. Kim, *Biomacromolecules*, 2008, **9**, 1698–1704.
34 M. Kim, Y. Shin, B. H. Hong, Y. J. Kim, J. S. Chun, G. Tae and Y. H. Kim, *Tissue Eng., Part C*, 2009, **16**, 1–10.
35 M. Kim, J. Lee, C. N. Jones, A. Revzin and G. Tae, *Biomaterials*, 2010, **31**, 3596–3603.
36 M. Kim, J. Y. Lee, S. S. Shah, G. Tae and A. Revzin, *Chem. Commun.*, 2009, 5865–5867.
37 C. N. Salinas and K. S. Anseth, *Macromolecules*, 2008, **41**, 6019–6026.
38 A. A. Aimetti, A. J. Machen and K. S. Anseth, *Biomaterials*, 2009, **30**, 6048–6054.
39 L. Gosey, R. Howard, F. Witebsky, F. Ognibene, T. Wu, V. Gill and J. Maclowry, *J. Clin. Microbiol.*, 1985, **22**, 803–807.

40 J. C. Y. Dunn, M. L. Yarmush, H. G. Koebe and R. G. Tompkins, *FASEB J.*, 1989, **3**, 174–179.
41 A. Revzin, R. J. Russell, V. K. Yadavalli, W.-G. Koh, C. Deister, D. D. Hile, M. B. Mellott and M. V. Pishko, *Langmuir*, 2001, **17**, 5440–5447.
42 B. V. Slaughter, S. S. Khurshid, O. Z. Fisher, A. Khademhosseini and N. A. Peppas, *Adv. Mater.*, 2009, **21**, 3307–3329.
43 M. P. Lutolf and H. M. Blau, *Adv. Mater.*, 2009, **21**, 3255–3268.
44 K. Matsumoto and T. Nakamura, *J. Biochem. (Tokyo)*, 1996, **119**, 591–600.
45 A. Suzuki, A. Iwama, H. Miyashita, H. Nakauchi and H. Taniguchi, *Development*, 2003, **130**, 2513–2524.
46 A. Revzin, P. Rajagopalan, A. W. Tilles, F. Berthiaume, M. L. Yarmush and M. Toner, *Langmuir*, 2004, **20**, 2999–3005.
47 S. N. Bhatia, U. J. Balis, M. L. Yarmush and M. Toner, *Biotechnol. Prog.*, 1998, **14**, 378–387.



 